Novel type II cell wall architecture in dichlobenil-habituated maize calluses

ARTICLE *in* PLANTA · FEBRUARY 2009

Impact Factor: 3.26 · DOI: 10.1007/s00425-008-0860-8 · Source: PubMed

Planta
DOI 10.1007/s00425-008-0860-8

ORIGINAL ARTICLE

Novel type II cell wall architecture in dichlobenil-habituated maize calluses

Hugo Mélida · Penélope García-Angulo · Ana Alonso-Simón · Antonio Encina · Jesús Álvarez · José Luis Acebes

Received: 3 October 2008 / Accepted: 10 November 2008

Abstract Growth of maize (*Zea mays* L.) callus-culture cells was inhibited using dichlobenil (2,6 dichlorobenzonitrile, DCB) concentrations ≥1 μM; I_{50} value for the effect on inhibited fresh weight gain was 1.5 μM. By increasing the DCB concentration in the culture medium, DCB-habituated cells became 13 times more tolerant of the inhibitor (I_{50}: 20 μM). In comparison with non-habituated calluses, DCB-habituated calluses grew slower, were less friable and were formed by irregularly shaped cells surrounded by a thicker cell wall. By using an extensive array of techniques, changes in type II cell wall composition and structure associated with DCB habituation were studied. Walls from DCB-habituated cells showed a reduction of up to 75% in cellulose content, which was compensated for by a net increase in arabinoxylan content. Arabinoxylans also showed a reduction in their extractability and a marked increase in their relative molecular mass. DCB habituation also involved a shift from ferulate to coumarate-rich cells walls, and enrichment in cell wall esterified hydroxycinnamates and dehydroferulates. The content of polymers such as mixed-glucan, xyloglucan, mannans, pectins or proteins did not vary or was reduced. These results prove that the architecture of type II cell walls is able to compensate for deficiencies in cellulose content with a more extensive and phenolic cross-linked network of arabinoxylans, without necessitating β-glucan or other polymer enhancement. As a consequence of this modified architecture, walls from DCB-habituated cells showed a reduction in their swelling capacity and an increase both in pore size and in resistance to polysaccharide hydrolytic enzymes.

Keywords Arabinoxylan · Callus culture · Cellulose · Dichlobenil · FTIR · Maize

Abbreviations

AIR	Alcohol insoluble residue
AGPs	Arabinogalactan proteins
AX	Arabinoxylan
CDTA	50 mM cyclohexane-*trans*-1,2-diamine-*N*,*N*,*N*′,*N*′-tetraacetic acid sodium salt
DCB	2,6-Dichlorobenzonitrile or dichlobenil
FTIR	Fourier transform infrared
GAX	Glucuronoarabinoxylan
H*x*	Dichlobenil-habituated calluses growing in *x* (μM) DCB
IDA	Immunodot assay
mAb	Monoclonal antibody
MPBS	PBS containing 4% fat-free milk powder
M_w	Average molecular weight
NH	Non-habituated calluses
PBS	0.1 M phosphate buffer saline
PCA	Principal component analysis
Rha	Rhamnose
snCR	Supernatant-cellulose residue
TFA	Trifluoroacetic acid

Introduction

Previous works have demonstrated the remarkable ability of plant cells to tolerate induced stresses (Iraki et al. 1989; Shedletzky et al. 1992; Encina et al. 2001, 2002) by changing

H. Mélida · P. García-Angulo · A. Alonso-Simón · A. Encina · J. Álvarez · J. L. Acebes (✉)
Área de Fisiología Vegetal, Facultad de CC., Biológicas y Ambientales, Universidad de León, 24071 León, Spain
e-mail: jl.acebes@unileon.es

Published online: 02 December 2008

their cell wall composition and structure. The herbicide DCB inhibits the polymerization of Glc into β-1,4-linked glucan and may also affect β-1,4-glucan crystallization at the plasma membrane, but has little or no short-term effect on other physiological processes (Delmer 1987). The habituation of cell cultures to cellulose biosynthesis inhibitors such as DCB, reflects the ability of cells to survive with a modified wall and is therefore a valuable experimental technique for gaining an insight into the plasticity of plant cell wall composition and structure (Vaughn 2002).

There are two types of cell walls in higher plants. Type I cell walls are found in dicots, gymnosperms and most monocots, and type II walls are found in graminaceous plants, along with the other commelinoid monocots (Carpita and Gibeaut 1993; Carpita 1996). Cellulose, a linear (1,4)-β-D-glucan, is the main load-bearing polysaccharide in both types of walls. In type I cell walls, xyloglucan interlaces the cellulose microfibrils, forming the main load-bearing network in the wall. This cellulose-xyloglucan framework is embedded in a matrix of pectic polysaccharides, homogalacturonan and rhamnogalacturonans I and II. Type I cell walls also contain minor amounts of protein, including basic proteins that can interact with the pectin network and with other proteins through intermolecular bridges. Type II cell walls are characterized by a reduction in xyloglucan, pectins and structural proteins, and by a higher content of other noncellulosic-polysaccharides, such as acidic xylans and 'mixed-linkage' (1,3)-(1,4)-β-D-glucan (Carpita et al. 2001). In the case of graminaceous cell walls, matrix pectins are mainly substituted by arabinoxylans and glucuronoarabinoxylan (GAX), which tether adjacent cellulose microfibrils. Also frequent in graminaceous cell walls is the presence of hydroxycinnamic acids (mainly ferulic and *p*-coumaric acid) ester linked to α-L-Ara residues of arabinoxylans (Ishii 1997). Hydroxycinnamic acids contribute to wall assembly by cross linking polysaccharides through the oxidative coupling of feruloyl residues (Fry et al. 2000).

Most DCB-habituated cultures belong to type I cell wall species, such as tomato (Shedletzky et al. 1990), tobacco (Shedletzky et al. 1992; Wells et al. 1994; Nakagawa and Sakurai 1998, 2001) and bean (Encina et al. 2001, 2002; Alonso-Simón et al. 2004). In type I cell walls habituated to DCB, there is a marked reduction in the amount of cellulose and hemicelluloses, whereas the quantity of esterified and unesterified pectins is increased. Moreover, in DCB-habituated BY-2 tobacco cells, pectins have been reported to be cross-linked with extensin to form the main cell wall network (Sabba et al. 1999). Other modifications have been associated with DCB habituation, such as the presence of a non-crystalline β-1,4-glucan tightly bound to cellulose, the accumulation of pectin-enriched cell wall appositions, a putative increase in the extent of pectin–xyloglucan cross-linking, reduced levels of arabinogalactan proteins (AGPs) and changes in the levels of extensin (Shedletzky et al. 1992; Encina et al. 2002; García-Angulo et al. 2006).

To date, barley cultures are the only cells with type II cell walls that have been habituated to DCB (Shedletzky et al. 1992). DCB-habituated barley cells showed a modified architecture: they contained a considerably reduced level of cellulose in the cell wall and this reduction was effectively compensated for by mechanisms (parallel to modifications) quite different to those observed in dicots, which implicated a higher proportion of β-glucan and a more extensive cross-linking between arabinoxylans, leading to walls with a reduction in pore size.

The present work addresses the selection and characterisation of a maize cell line able to grow in the presence of lethal concentrations of DCB. The results show a novel type II cell wall architecture accompanied by unique cell wall properties.

Materials and methods

Cell cultures

Maize callus cultures (*Zea mays* L., Black Mexican sweetcorn, donated by Dr. S. C. Fry, Institute of Molecular Plant Sciences, University of Edinburgh, UK) from immature embryos were grown in Murashige and Skoog media (Murashige and Skoog 1962) supplemented with 9 μM 2,4-D at 25°C under light (Lorences and Fry 1991), and subcultured monthly.

Habituation to dichlobenil

Calluses weighing 1.0 ± 0.1 g were cultured in dichlobenil (supplied by Fluka), in concentrations ranging from 0.01 to 100 μM. DCB was dissolved in dimethyl sulfoxide (DMSO), which did not affect cell growth at this range of concentrations. The cultures were incubated for 30 days, weighed (FW) and heated at 60°C until constant weight was achieved (DW). Growth was expressed as relative increase in FW and the I_{50} was calculated as the concentration of DCB able to inhibit weight increase by 50% with respect to the control.

Calluses were habituated to growth in different DCB concentrations by stepwise transfers with gradual increments of DCB, beginning at 2 μM. At least three subcultures of approximately 30 days were performed between each increase in the DCB concentration. Growth curves were obtained for habituated calluses growing in DCB and for non habituated calluses, by measuring the relative increase in FW every 4–6 days.

Electron microscopy

Callus pieces were fixed in 2.5% (w/v) paraformaldehyde in 0.1 M sodium phosphate buffer, pH 7.4, and post-fixed with OsO_4 in the same buffer. The samples were dehydrated in an increasing series of ethanol concentrations and embedded in LR White Resin (London Resin Co. Ltd, Basingstoke, UK). This was done by sequentially placing the segments in ethanol and resin (2:1, v/v) for 8 h, ethanol and resin (1:2, v/v) for 8 h, and in pure resin. The samples were transferred to a gelatin capsule, fresh resin added, and the resin polymerized at 60°C for 48 h. Blocks were sectioned (1.5–2 µm thick) with a LKB 2088 ultramicrotome. Ultrathin sections were mounted on copper grids and post-stained with uranyl acetate and lead citrate before observation with a JEOL (JEM-1010) electron microscope. Cell wall thickness was determined by random measurement of cell walls from 30 cells.

Immunolocation

For the immunolocation of cell wall components, the gelatine capsules were polymerized at 37°C for 5 days. Sections were obtained (1.5–2 µm thick) and applied to multi-well slides (ICN Biomedicals, Cleveland, OH, USA) coated with Vectabond reagent (Vector Laboratories, Burlingame, CA, USA). Sections were incubated for 2 h with 0.1 M phosphate buffer saline (PBS) (0.14 M NaCl, 2.7 mM KCl, 7.8 mM Na_2HPO_4 12 H_2O, 1.5 mM KH_2PO_4, pH 7.2) containing 4% fat-free milk powder (MPBS) with the primary antibody at a 1/10 dilution. After washing exhaustively with PBS, the sections were incubated in darkness for 2 h with a 1/100 dilution of an antirat immunoglobulin G linked to fluorescein isothiocyanate (Sigma) in MPBS at room temperature. Finally, sections were washed with PBS and mounted in a glycerol/PBS-based antifade solution (Citifluor AF1; Agar Scientific, London, UK) and observed using a Nikon Eclipse-TS100 microscope with epifluorescence irradiation. Cellulose was localized in sections using calcofluor white (fluorescent brightener 28, Sigma). Xylans were probed by using mAb LM10 (specific for 1,4-β-xylans) (McCartney et al. 2005) and LM11 (for xylans and arabinoxylans) (McCartney et al. 2005). Cell wall esterified feruloyl groups were probed with LM12, a new antibody developed at the Paul Knox laboratory (Leeds University, UK). AGPs were probed with mAbs LM2 (Smallwood et al. 1996), MAC207 (Pennell et al. 1989) and JIM8 (Pennell et al. 1991).

Preparation and fractionation of cell walls

Calluses collected during growth in the early stationary phase were frozen and homogenized with liquid nitrogen and treated with 70% ethanol for 5 days at room temperature. The suspension was then centrifuged and the pellet washed with 70% ethanol (×6), acetone (×6), and air dried, in order to obtain the alcohol insoluble residue (AIR). The AIR was treated with 90% DMSO for 8 h at room temperature (×3) and then washed with 0.01 M phosphate buffer pH 7.0 (×2). The washed AIR was then treated with 2.5 U ml^{-1} α-amylase obtained from porcine pancreas (Sigma type VI-A) in 0.01 M phosphate buffer pH 7.0 for 24 h at 37°C (×3). The suspension was filtered through a glass fibre, and the residue washed with 70% ethanol (×6), acetone (×6), air dried and then treated with phenol–acetic–water (2:1:1, by vol.) for 8 h at room temperature (×2). This was finally washed with 70% ethanol (×6), acetone (×6) and air dried in order to obtain the cell walls.

For cell wall fractionation, dry cell walls were extracted at room temperature with 50 mM cyclohexane-*trans*-1,2-diamine-*N*,*N*,*N*′,*N*′-tetraacetic acid sodium salt (CDTA) at pH 6.5 for 8 h and washed with distilled water. The residue was retreated with 0.1 M KOH for 2 h (×2) and washed with distilled water. Then 4 M KOH was added to the residue for 4 h (×2), and washed again with distilled water. The extracts were neutralized with acetic acid, dialysed and lyophilized, representing CDTA, KOH-0.1 M and KOH-4 M fractions, respectively. The residue after 4 M KOH extraction was suspended in water, adjusted to pH 5 with acetic acid, and dialysed. After centrifugation, the supernatant was filtered and lyophilized; this was referred to as the supernatant-cellulose residue (snCR) fraction. The residue was hydrolysed for 2.5 h at 120°C with 2 M trifluoroacetic acid (TFA), and after centrifugation, the supernatant was lyophilized and referred to as the TFA fraction.

Cell wall analyses

Cellulose was quantified in crude cell walls with the Updegraff method (Updegraff 1969), using the hydrolytic conditions described by Saeman et al. (1963) and quantifying the glucose released by the anthrone method (Dische 1962).

Tablets for Fourier transform infrared (FTIR) spectroscopy were prepared in a Graseby-Specac press from small samples (2 mg) of cell walls mixed with KBr (1:100, w/w). Spectra were obtained on a Perkin–Elmer instrument at a resolution of 1 cm^{-1}. A window of between 800 and 1,800 cm^{-1}, containing information about characteristic polysaccharides, was selected in order to monitor cell wall structure modifications. All spectra were normalized and baseline-corrected with Spectrum v 5.3.1 (2005) software, by Perkin–Elmer. Data were then exported to Microsoft Excel 2003 and all spectra were area-normalized. Cluster analysis was performed using the Ward method, and the Pearson coefficient was selected as distance measurement. Principal component analysis (PCA) was performed using a maximum of five principal components. All analyses were carried out using the Statistica 6.0 software package.

The total sugar content of each fraction was determined by the phenol–sulfuric acid method (Dubois et al. 1956) and expressed as the glucose equivalent. Uronic acid content was determined by the *m*-hydroxydiphenyl method (Blumenkrantz and Asboe-Hansen 1973) using galacturonic acid as a standard. Xyloglucan content was obtained by the iodine-staining method (Kooiman 1960). Neutral sugar analysis was performed as described by Albersheim et al. (1967). Lyophilized samples of each fraction were hydrolysed with 2 M TFA at 121°C for 1 h and the resulting sugars were derivatized to alditol acetates and analysed by gas chromatography (GC) using a Supelco SP-2330 column.

The quantification of (1 → 3,1 → 4)-β-glucans was carried out using a direct and specific enzymatic assay with the (1 → 3,1 → 4)-β-glucan endo-hydrolase from *Bacillus subtilis* (McCleary and Codd 1991).

To measure cell wall degradability, cell walls were hydrolysed (5 mg ml^{-1}) in a mixture of cellulase R-10 (0.1%), macerozyme R-10 (0.1%) and purified driselase (0.01%) dissolved in sodium acetate 20 mM (pH 4.8) (Grabber et al. 1998). Aliquots were taken at 2, 6, 24, 48 and 72 h, clarified by centrifugation and assayed for total sugars following the method described by Dubois et al. (1956).

In vitro measurement of cell wall swelling examined the relative volume increase that took place after re-hydrating dry walls in 8 mm diameter tubes (Encina et al. 2002).

For amino acid analysis, cell walls were hydrolysed in 6 N HCl at 110°C for 24 h, filtered through Whatman paper and dried by speed-vac. Soluble amino acids were derivatized by using phenyl isothiocyanate, and then separated, identified and quantified following the method described by Alonso et al. (1994). Total protein content was estimated by summation of the amounts of amino acids measured.

Assay of esterified phenolic acids

Cell walls (10 mg) were treated in the dark with 1 M NaOH, at room temperature for 12 h to saponify phenolic esters. The solution was acidified by addition of TFA and partitioned against ethyl acetate (×2). The ethyl acetate phases were pooled and mixed with a solution containing 1% 8,5-diferulic acid, 5,5-diferulic acid, 8-*O*-4 diferulic acid, *p*-coumaric acid and ferulic acid as internal markers, then vacuum-dried and re-dissolved in propan-1-ol. Portions of the propanol solution were subjected to TLC on silica-gel in benzene/acetic acid (9:1, v/v).

Gel-permeation chromatography

Hemicellulosic fractions were size-fractionated by gel-permeation chromatography on Sepharose CL-4B (120–125 ml bed-volume in a 1.5 cm diameter column) in pyridin: acetic acid:water (1:1:98, by vol.) at 0.3 ml min^{-1}. The column was calibrated with commercial dextrans of known weight-average relative molecular mass, and hemicellulose average molecular weight (M_w) was obtained using the $K_{av(1/2)}$ method (Kerr and Fry 2003), with the calibration curve [$\log M_w = -4.999K_{av(1/2)} + 7.849$] obtained for this column. The M_w estimates are nominal rather than absolute because of conformational differences between dextran and hemicelluloses.

Porosity measurements

Porosity was determined using the technique developed by Baron-Epel et al. (1988). Cells at the logarithmic stage of growth were resuspended in 10 mM 2-amino-2(hydroxymethyl)-1,3-propanediol (Tris; pH 5.5), 10 mM $CaCl_2$, and 0.5 M mannitol in order to induce plasmolysis. They were then suspended in a medium with fluorescein isothiocyanate-dextrans (Sigma) at a final concentration of 500 µg ml^{-1}. Fluorescence was observed using a Nikon Eclipse-TS100 epifluorescent microscope equipped with a Nikon B-2 A filter (450–490 nm excitation, 510 nm dichroic mirror and 520 nm barrier filter).

Immunodot assays

For immunodot assays (IDAs), aliquots of 1 µl from KOH-0.1 M and KOH-4 M fractions containing 5 µg of total sugars were spotted onto nitrocellulose membrane (Schleicher & Schuell, Dassel, Germany) as a replicated dilution series and probed as described by Willats et al. (1999) and García-Angulo et al. (2006). All primary antibodies (JIM8, LM11 and LM12) were used at 1/5 dilutions.

Results

Effect of DCB on callus cultures and habituation

In order to determine the effect of DCB on maize callus cultures we tested its inhibitory effect on fresh weight gain (Fig. 1). The weight gain of non-habituated calluses (NH) was slightly stimulated at low concentrations of DCB, but was diminished by DCB concentrations equal to or higher than 1 µM. The I_{50} was 1.5 µM for FW.

Maize calluses' tolerance to lethal concentrations of DCB was achieved by gradually increasing the concentration of the inhibitor in the culture medium, beginning at 2 µM. After 12 subcultures of an average of 30 days each, maize cells were capable of growth in 12 µM DCB (H12). As for non-habituated cell cultures, a stimulation of FW gain was observed for the lowest DCB concentration used. In the case of H12 cells, the I_{50} value for FW inhibition gain was approximately 13 times higher (20 µM).

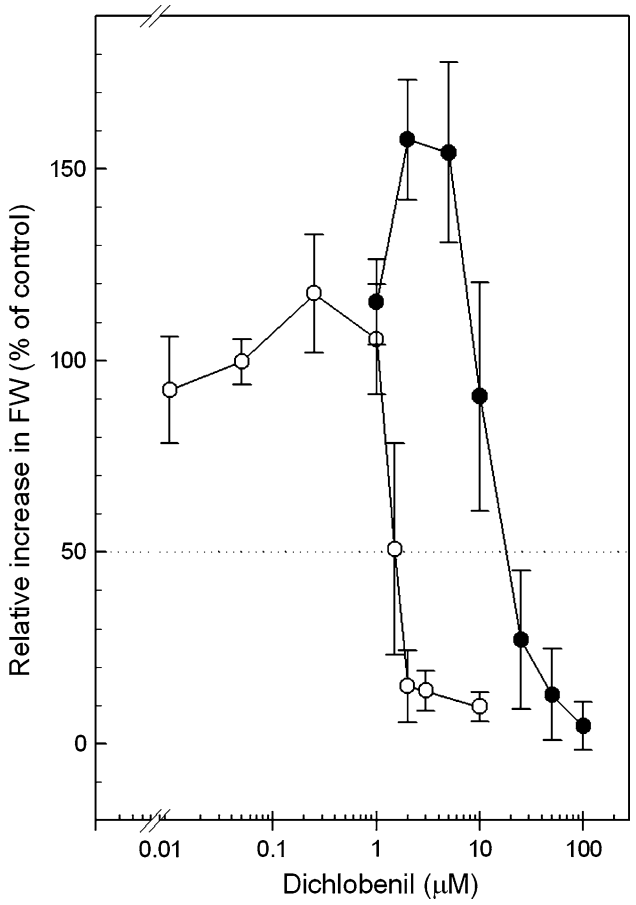

Fig. 1 Growth inhibition curves of maize calluses by increasing concentrations of DCB after 30 days of culture. *Open circle* non-habituated (NH) calluses, *filled circle* habituated to 12 μM DCB (H12) calluses. Values are mean ± SD of six measurements

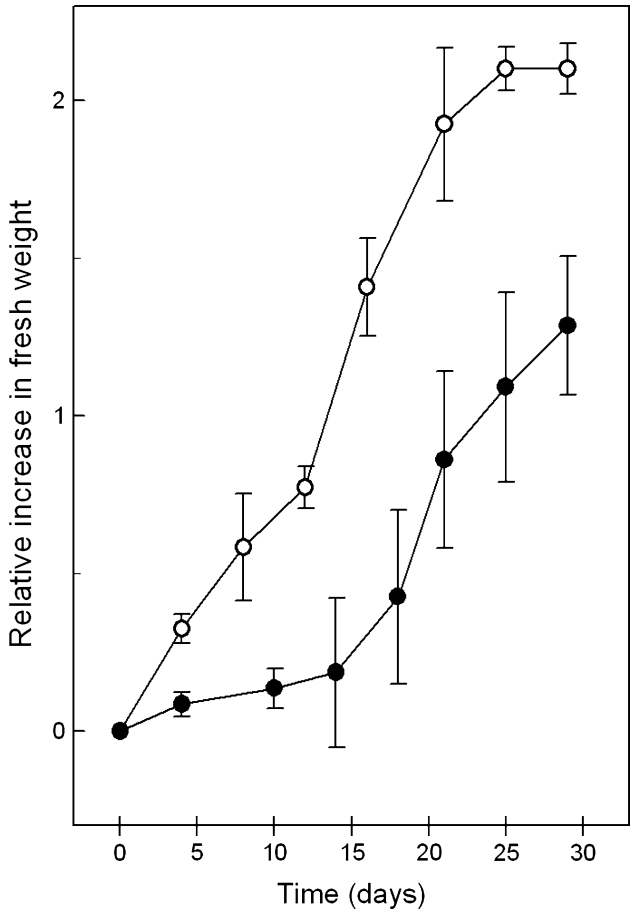

Fig. 2 Relative increase in FW of maize calluses during the culture. *Open circle* NH calluses, *filled circle* H12 calluses. Values are mean ± SD of six measurements

Characterization of callus cultures and cells

Habituated cells (H12) growing on DCB had longer lag phases and less FW was accumulated (Fig. 2). Moreover, H12 cells had a higher DW/FW ratio and cell wall yield per DW than non-habituated ones (Table 1).

H12 calluses were darker and less friable, and formed hard protuberances during growth. H12 cells were rather irregular (Fig. 3b) in comparison with NH cells, which were more or less isodiametrically shaped (Fig. 3a). Groups of cells with thicker walls, apparently arising from the same cell, were frequent in habituated cell preparations (Fig. 3b).

Cell wall analysis

Ultrastructure and porosity

NH cells were surrounded by a uniform cell wall (Table 1), in comparison with H12 cell walls, which were less uniform (Fig. 3d) and 1.6 times thicker than those from NH ones (Fig. 3c). H12 cell walls (Fig. 3b) were less calcofluor-stained than NH cell walls (Fig. 3a), probably due to the reduction in cellulose.

H12 cell walls half-swelled compared with NH ones (Table 1), but porosity increased (Table 2); limiting diameter of dextrans to be excluded for cell walls increased from 6.6 to 12 nm when NH and H12 cells were compared, although long incubation times were required by 9-nm-diameter dextrans to go through H12 cell walls.

FTIR spectroscopy

Changes in the cell wall during the habituation process were monitored by FTIR spectroscopy. Twelve representative FTIR cell wall spectra from non-habituated and habituated to different DCB concentrations calluses were analysed. FTIR spectra from habituated cell walls showed differences in wavenumbers corresponding to cellulose, phenolic components, arabinose and proteins. They also showed variations in the main phenolic linkage: ester bonds (data not shown). To elucidate differences among these spectra, a multivariate analysis was performed (Fig. 4a).

Table 1 Variation of some characteristics of cell lines during habituation

Cell type	DW/FW[a]	Wall DW/callus DW[a]	Cell wall thickness (μm)[b]	Cell wall swelling[c]
NH	0.0399 ± 0.0074	0.2409 ± 0.0052	0.1344 ± 0.0343	1.72 ± 0.19
H12	0.0623 ± 0.0100	0.5451 ± 0.0029	0.2137 ± 0.1113	0.80 ± 0.13

Cell wall swelling is represented as relative increase in volume

Values are mean ± SD of [a]10, [b]30 or [c]6 measurements

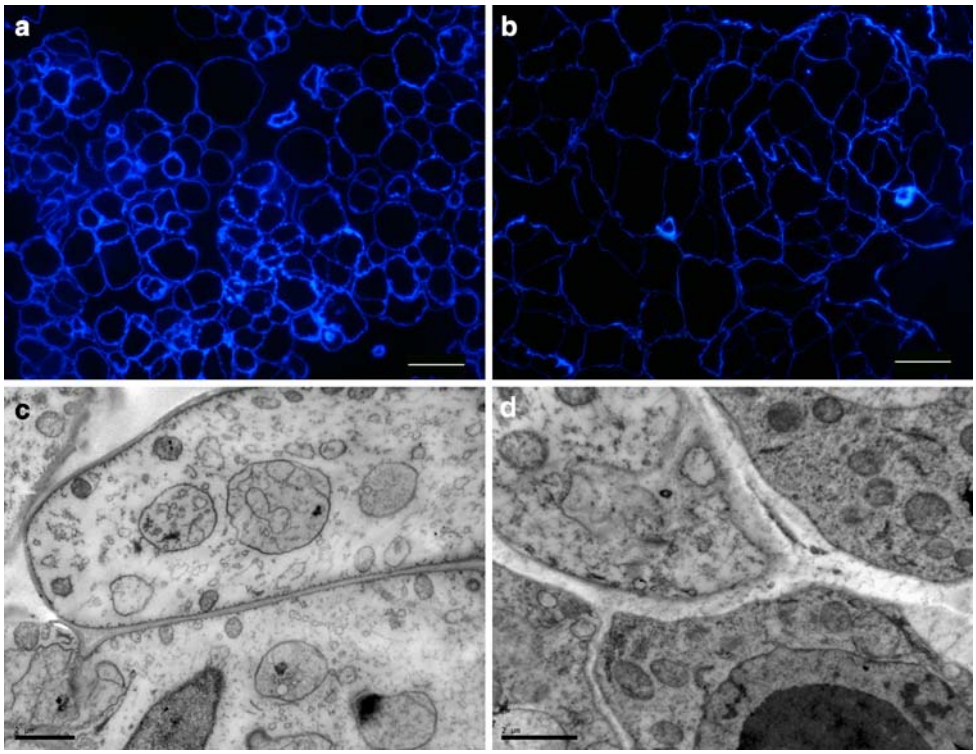

Fig. 3 Sections of NH (**a**) and H12 (**b**) callus calcofluor stained. Ultra-structural appearance of cell walls of NH (**c**) and H12 (**d**) callus. *Bars* 50 μm (**a**, **b**), 2 μm (**c**, **d**)

Table 2 Comparison of porosities of NH and H12 cell walls

Molecular mass of FTIC-dextrans (kDa)	Stokes diameters (nm)	NH	H12
10	4.6	+[a], +[b], +[c]	+, +, +
20	6.6	−, −, −	±, +, +
40	9	−, −, −	−, −, +
70	12	−, −, −	−, −, −

+, Dye penetrates >80% of cell walls; −, dye penetrates <20% of cell walls

[a] Measurement at 30 min

[b] Measurement at 60 min

[c] Measurement at 120 min

Principal components 1 and 3 (PC1 and PC3) were used to discriminate between groups of spectra. Cell walls from non-habituated cells were located on the negative side of PC1 and PC3; when the habituation process began, the points corresponding to the cell walls of habituated calluses were displaced to the positive side of PC1 and PC3. Generally, the more habituated the calluses, the more positive the PC1 and PC3 placement. NH treated for short periods with 6 μM DCB displaced to the positive side of PC1 but to the negative side of PC3, suggesting that the changes in cell walls promoted by DCB were different in habituated and non-habituated cells.

PC3 was more discriminative than PC1. PC3 loading factor plot (Fig. 4b) showed a negative area at the fingerprint region 950–1,175 cm^{-1}, indicative of polysaccharides. In this area, correlated negative peaks could be identified, mainly at 1,160, 1,105, 1,060 and 1,040 cm^{-1}, indicative of cellulose (Carpita et al. 2001). Also, two major protein negative absorbances at 1,550 and 1,650 cm^{-1} were detected. Thus, spectra located at the negative side of PC3, i.e. NH-seemed to have a relatively higher amount of polysaccharides—mainly cellulose—and proteins. In contrast, PC3 showed positive peaks at several wavenumbers indicative of aromatic rings: 1,630 (ring conjugated C=C), 1,600 (aryl ring stretching symmetric), about 1,500 (phenolic ring), and 1,425, 1,180 and 843 (aromatic C–H out of bending) cm^{-1}. The peak at 856 cm^{-1} corre-

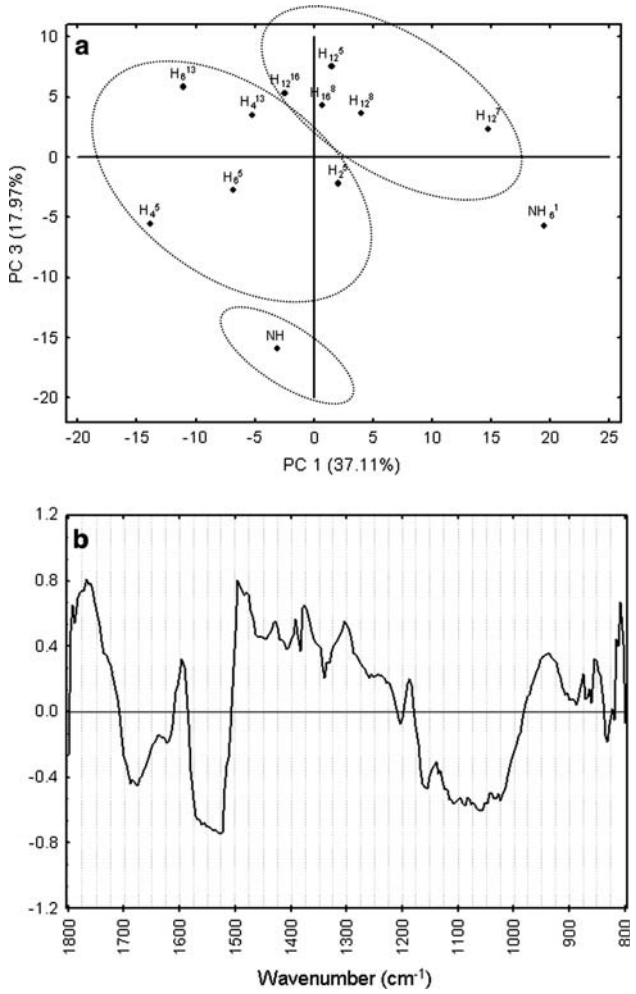

Fig. 4 **a** Principal component analysis of callus spectra. A plot of the first and third PCs is represented based on the FTIR spectra of non-habituated (NH) and habituated calluses (H_x^n, *x* DCB concentration (μM), *n* number of subcultures in that concentration). NH_6^1, non-habituated calluses treated for 5 days with 6 μM DCB. **b** Factor loadings for PC3

sponds to furanoid ring (i.e. Ara*f*); and 1,381, 1,376 and 1,312 cm^{-1} correspond to polysaccharides (Kacurakova et al. 1999).

Summing up, the expected changes in cellulose were accompanied by changes in other components, like arabinose, phenolics and proteins, and multivariate analyses demonstrated that during habituation, cell walls underwent gradual modifications.

Cellulose content

The increase in DCB concentration during the habituation process caused a reduction in cellulose content (Fig. 5). This reduction correlated with the habituation level until H6. H12 walls had about 25% of the amount of cellulose found in their NH counterpart, with no further change as the level of tolerance increased.

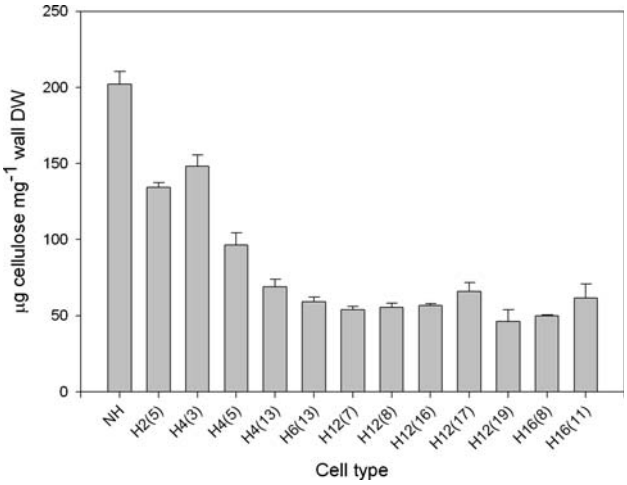

Fig. 5 Cellulose content of cell walls isolated from calluses at different DCB tolerance levels. NH, non-habituated callus; $H_x(n)$, habituated callus, where *x* DCB concentration (μM), and *n* number of subcultures in that concentration. Values are mean ± SD of three measurements

Cell wall fractionation and sugar analysis

Cell wall fractionation (Fig. 6) showed that the bulk of polysaccharides were extracted from the cell walls by alkali treatment: KOH-0.1 M and KOH-4 M fractions. These two fractions, plus the TFA fraction, accounted for about 90% of the total cell-wall sugar content. A net increase in the yield of sugars per dry cell wall weight was observed during the habituation to DCB (0.38 in NH vs. 0.48 in H12). This effect was mainly due to a notable increase in polysaccharides extracted with strong alkali (KOH-4 M fraction). The total amount of CDTA-extracted polysaccharides was reduced during habituation to DCB, while a slight increase in polysaccharides tightly bound to cellulose (TFA and snCR fractions) was detected. As regards the polysaccharides extracted with diluted alkali (KOH-0.1 M fraction), an increase in intermediate levels of tolerance was measured.

GC analysis of cell wall fractions (Fig. 7) showed that KOH-0.1 M and KOH-4 M fractions were composed mainly of Ara and Xyl followed by uronic acids, Gal and Glc, whereas minor fractions such as CDTA and snCR were composed of the same monosaccharides and enriched with uronic acids. The detected variations in the amount of sugar extracted in KOH-0.1 M and KOH-4 M and TFA fractions were paralleled by variations in Ara and Xyl. Especially important is the gradual enrichment in Ara and Xyl found in KOH-4 M and TFA fractions throughout the habituation process. The reduced levels of Glc reflect the poor levels of xyloglucan and mixed-linked glucan in these cell walls. These two polysaccharides are even further reduced after habituation (Table 3).

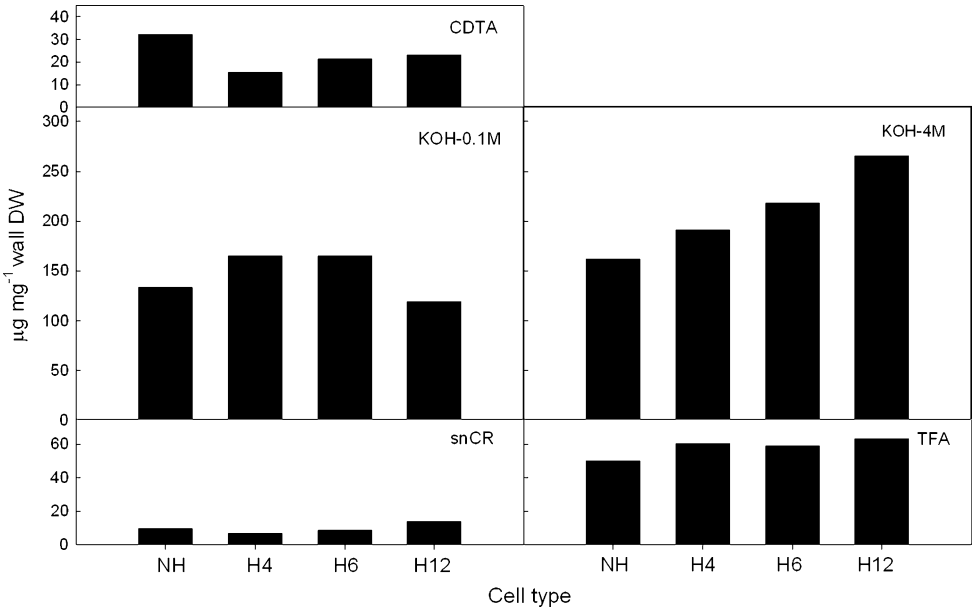

Fig. 6 Total sugars in cell wall fractions at different DCB habituation levels. NH, non-habituated calluses; H*x*, habituated calluses where *x* DCB concentration (µM). Calluses with at least eight subcultures in medium containing the indicated concentration of DCB were used. Results came from a representative experiment

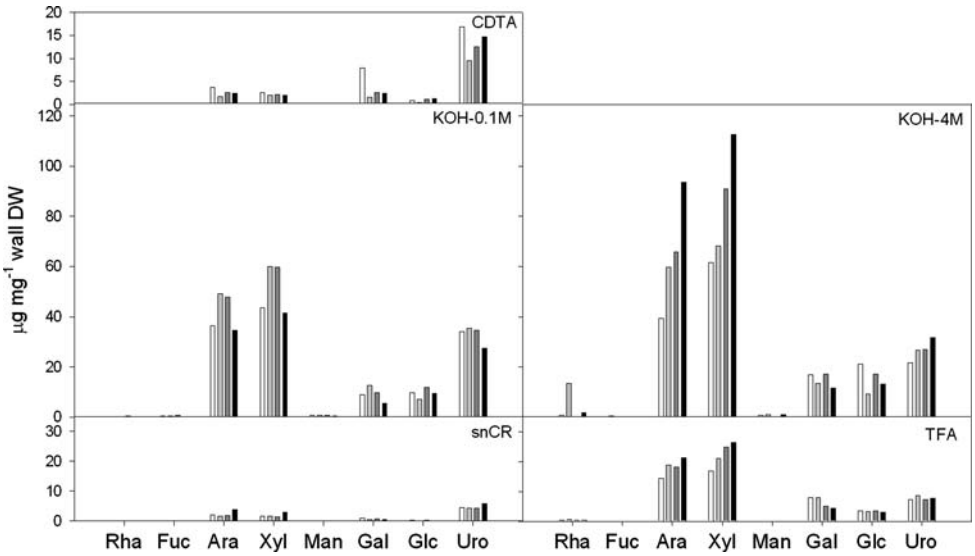

Fig. 7 Sugar composition of fractions from cell walls of NH (*open square*), H4 (*light grey square*), H6 (*dark grey square*) and H12 (*black square*) calluses. *Rha* rhamnose, *Fuc* fucose, *Ara* arabinose, *Xyl* xylose, *Man* mannose, *Gal* galactose, *Glc* glucose, *Uro* uronic acids

Table 3 Xyloglucan (XyG) and mixed-linked glucan (MLG) content of KOH fractions and crude cell walls, respectively

Cell type	XyG		MLG
	KOH-0.1 M	KOH-4 M	
NH	2.84 ± 0.19	19.93 ± 0.42	2.75 ± 0.12
H12	1.63 ± 0.07	12.01 ± 0.63	1.92 ± 0.09

Data units: µg mg^{-1} wall DW. Values are mean ± SD of three measurements

Therefore, a net enrichment in arabinoxylans, concomitant with a reduction in cellulose, was the main change observed in cell wall composition involved in DCB habituation.

Gel-permeation chromatography

Gel-permeation chromatography showed differences in the molecular mass of hemicellulosic polysaccharides (Table 4). Interesting changes took place in the 4 M KOH extractable polysaccharides (Fig. 8). At low and medium habituation levels the M_w of 4 M KOH extracted polysaccharides was reduced, but in the H12 fraction a significant increase took place; there was a net shift towards higher molecular masses and a new peak appeared close to the void volume. This peak was isolated and GC-analysed; Ara and Xyl accounted for about 78% (data not shown). In the KOH-0.1 M fractions, the opposite tendency was observed: H4 and H6 increased, whilst H12 increased only slightly (Table 4).

Table 4 Average molecular weight (M_w) of the hemicellulosic fractions

Cell type	KOH-0.1 M (kDa)	KOH-4 M (kDa)
NH	80.28	748.85
H4	446.11	298.18
H6	467.34	467.16
H12	134.75	2612.35

The M_w was obtained using the $K_{av(1/2)}$ method, with the calibration curve [$\log M_w = -4.999K_{av(1/2)} + 7.849$] obtained for this column

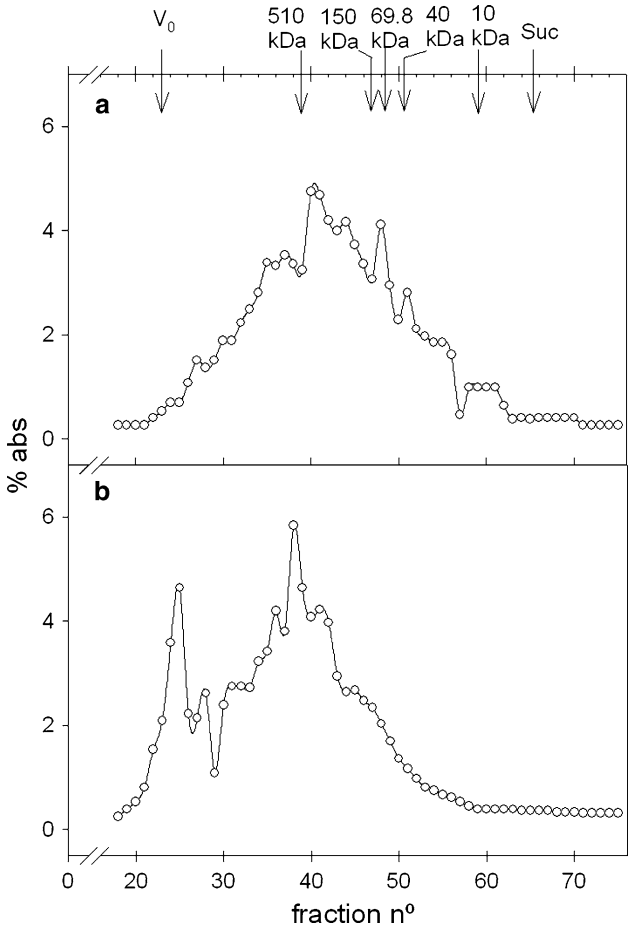

Fig. 8 Elution profiles of 4 M-KOH-extractable polysaccharides from NH (**a**) and H12 (**b**) calluses. *Markers* blue dextran (V_0), dextrans of 510, 150, 69.8, 40, 10 kDa, and sucrose

Phenolics analysis

Saponified phenolics were TLC subjected (Fig. 9). The main phenolic component released from NH cell walls was ferulic acid, followed by *p*-coumaric and 5,5-diferulic acid. Habituation to DCB clearly involved a shift from ferulic acid to *p*-coumaric acid enriched cell walls. Habituated cell walls also showed increased levels of 5,5, 8-*O*-4 and 8,5 diferulic acids and low R_f material probably corresponding to dimers, trimers or larger coupling products. The difference between mild and strong alkali treatment was not qualitative but quantitative both in NH and in H12 (data not shown).

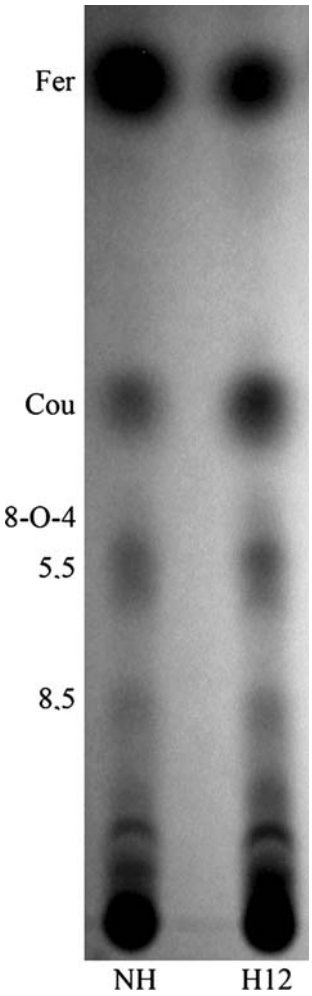

Fig. 9 TLC of phenolics alkali extracted from NH and H12 maize walls. Abbreviations in the TLC panel represent the position of migration of the following standards: (8,5), 8,5-di-ferulic acid; (5,5), 5,5-di-ferulic acid; (8-*O*-4), 8-*O*-4 di-ferulic acid; (Cou), *p*-coumaric acid; (Fer), ferulic acid

Protein content and amino acid composition of the cell wall

DCB habituation changed protein content and amino acid composition of cell walls (Table 5). The insoluble protein content of cell walls was reduced in H12 cells by 30%. Expressed as a percentage of total amino acid, an increase in Glu and a reduction in Asp, Pro, Tyr, and Phe was detected in H12 cell walls.

Cell wall immunoanalysis

Due to increased levels of arabinoxylans in habituated cells, cell walls were probed with LM10 (McCartney et al. 2005),

Table 5 Amino acid composition (mol%) of insoluble protein from cell walls

Amino Acid	Cell type	
	NH	H12
Asp	11.4	2.9
Glu	11.4	36.9
Hyp	2.3	1.7
Asn	4.2	1.1
Ser	0.9	0.6
Thr	3.0	2.6
Ala	10.0	7.6
Pro	3.7	1.7
Tyr	3.1	1.7
Val	18.3	15.4
Ile	3.7	3.4
Leu	4.5	5.5
Phe	6.5	3.7
Trp	9.1	6.8
Lys	3.0	4.5
Arg	4.8	3.6

Values represent the mean of two independent assays

specific for 1,4-β-xylans, and LM11 (McCartney et al. 2005) specific for xylans and arabinoxylans. LM11 epitope was only found in habituated cell walls (Fig. 10b), although the IDA showed that NH cell walls can also bind it, but clearly to a lesser degree (Fig. 11b, e). According to fractionation results, most LM11 labelling appears in the 4 M-KOH fractions. No epitopes for LM10 were found in any of the cell types probed (data not shown). Cell wall esterified feruloyl groups were probed with LM12 (Fig. 10c, d). LM12 epitope was found in both cell types, but the immunofluorescent labelling in H12 cells (Fig. 10d) seemed weaker than that of NH (Fig. 10c). IDA for LM12 (Fig. 11c, f) showed that most labelling was found in 0.1 M-KOH fractions, and was reduced in habituated ones.

In the case of AGPs, different results were found depending on the antibody used. Whereas no type of cell bound MAC207, both control and habituated cells bound LM2 (data not shown). The difference was in JIM8, where only NH cells bound it (Fig. 10e). IDAs for this antibody (Fig. 11a, d) showed that habituated cells had progressively lesser labelling as habituation level increased.

Cell wall degradability

NH cell walls were quickly and completely degraded by cell wall digesting enzymes, with a total sugar yield of 821 and 1,000 μg mg^{-1} being released after 6 and 72 h of incubation, respectively (Fig. 12). In the hydrolytic conditions assayed, H12 cell walls were significantly more resistant to enzymatic degradation than NH cell walls, and a reduction of 40% in the yield of sugars released was measured after 72 h of incubation. Thus, the modifications that take place during habituation seem to build a strengthened cell wall in response to DCB.

Discussion

Maize calluses have been successfully habituated to lethal DCB concentrations, by gradually increasing the concentration of the inhibitor in the culture medium. This habituation procedure led to progressive widespread changes in callus growth and morphology: habituated calluses grew more slowly, formed hard protuberances, and were darker and harder. Their cells were more irregularly shaped, with a thicker and more irregular cell wall, which contributed to a higher dry weight in proportion to total dry weight. All these characteristics resembled those of other previously described cellulose-inhibitor-habituated cell cultures, such as DCB-habituated tomato cell suspensions (Shedletzky et al. 1990), and DCB- or isoxaben-habituated bean calluses (Díaz-Cacho et al. 1999; Encina et al. 2001).

As far as we know, only one other example of a type II cell wall species (barley) habituated to DCB has been reported to date (Shedletzky et al. 1992). DCB-habituated barley cells also showed a reduced growth rate. However, they showed net differences when compared to DCB-habituated maize cells: their cells were not larger than controls, were more isodiametrically-shaped and did not possess thicker cell walls. These differences could be explained—at least partially—by taking into account the different callogenic origin of both cultures. Barley cell cultures were generated from endosperm tissue (Shedletzky et al. 1992) whereas our maize cells were generated from immature embryos.

It has been suggested previously that the mechanism of habituation to DCB and other cellulose biosynthesis inhibitors relies on the ability of the habituated cells to divide and expand under conditions where cellulose synthesis is inhibited. In fact, maize and barley habituated cultures showed cellulose reductions of up to 70–75%. Both DCB-habituated barley and maize cell cultures compensated for the reduction in cellulose with a higher quantity of hemicellulosic polysaccharides, while uronic acids hardly varied. However, the increment in hemicellulosic polysaccharides had different origins in the cultures: in DCB-habituated barley cells, the only polysaccharide where the proportion rose was mixed-linked glucan, which increased its content fourfold, to reach more than 100 μg mg^{-1} cell wall. However in DCB-habituated maize cells, the reduction in cellulose was paralleled by a net increase in arabinoxylans, whereas other hemicelluloses such as β-glucan and xyloglucan were reduced. Thus, we have proven for the first time that the architecture of type II cell walls is able to compensate for

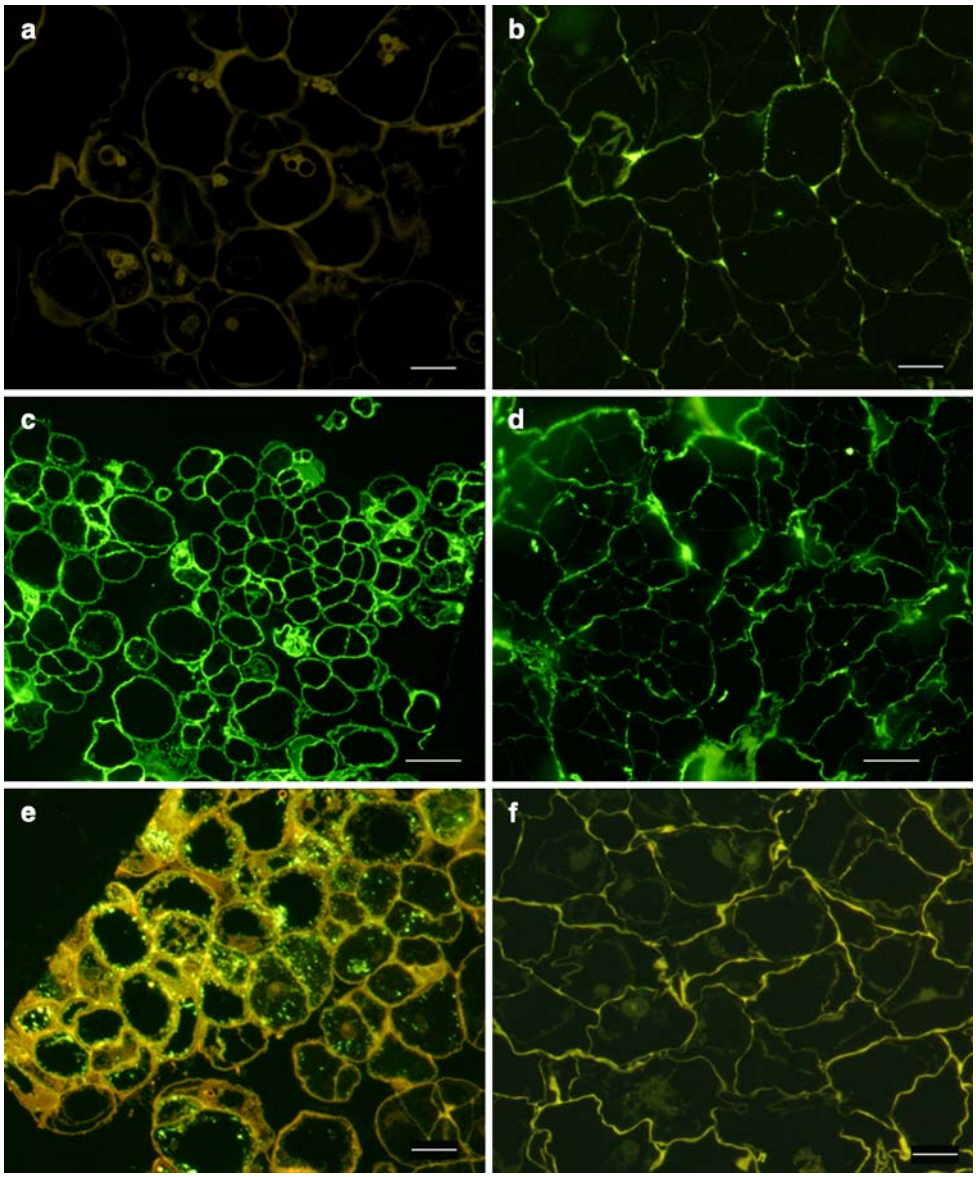

Fig. 10 Immunofluorescent localization of (1 → 4)-β-D-xylan/arabinoxylan (LM11: **a**, **b**), feruloylates (LM12: **c**, **d**) and arabinogalactan-proteins (JIM8: **e**, **f**) of NH (**a**, **c**, **e**) and H12 (**b**, **d**, **f**) maize cells. *Bars* 20 μm (**a**, **b**, **e**, **f**), 50 μm (**c**, **d**)

deficiencies in cellulose content without requiring a mixed glucan increment. In this modified architecture, the reduction in cellulose content is compensated for mainly by an increment in arabinoxylan content, whose characteristics appear modified in comparison with those of non-habituated cells.

The enhanced arabinoxylan content of habituated cells was appreciable by probing with LM11, an antibody that binds to xylan or arabinoxylan with a low degree of substitution (McCartney et al. 2005). LM11 labelling of habituated cell walls was much more intense than in non-habituated cell walls. Additionally, the LM11-binding pattern of habituated cell walls shows that LM11 epitopes are mainly localized in cell junctions, in thicker cell walls and in dispersed cell wall areas, pointing to particular cell wall strengthening in some areas.

Arabinoxylans in DCB-habituated maize cells also showed differences in extractability, mean molecular mass and in the formation of phenolic bridges, when compared with non-habituated cells.

Cell wall fractionation, GC and IDA for LM11-epitopes of KOH-extracted polysaccharides confirmed the reported net increase of AX in DCB-habituated cells, and showed a shift of AX from mild-alkali-extracted fractions (0.1 M-KOH) to strong-alkali-extracted fractions (4 M-KOH) and cellulose tightly bound fraction (TFA), pointing to a more extensive cross-linked hemicellulosic network.

Strong-alkali-extracted AX from habituated cell walls also showed a significant increase in M_w. This result can be explained by an increase in the polymerization and/or substitution degree of AX. This is an interesting result taking into account the fact that a major factor controlling AX

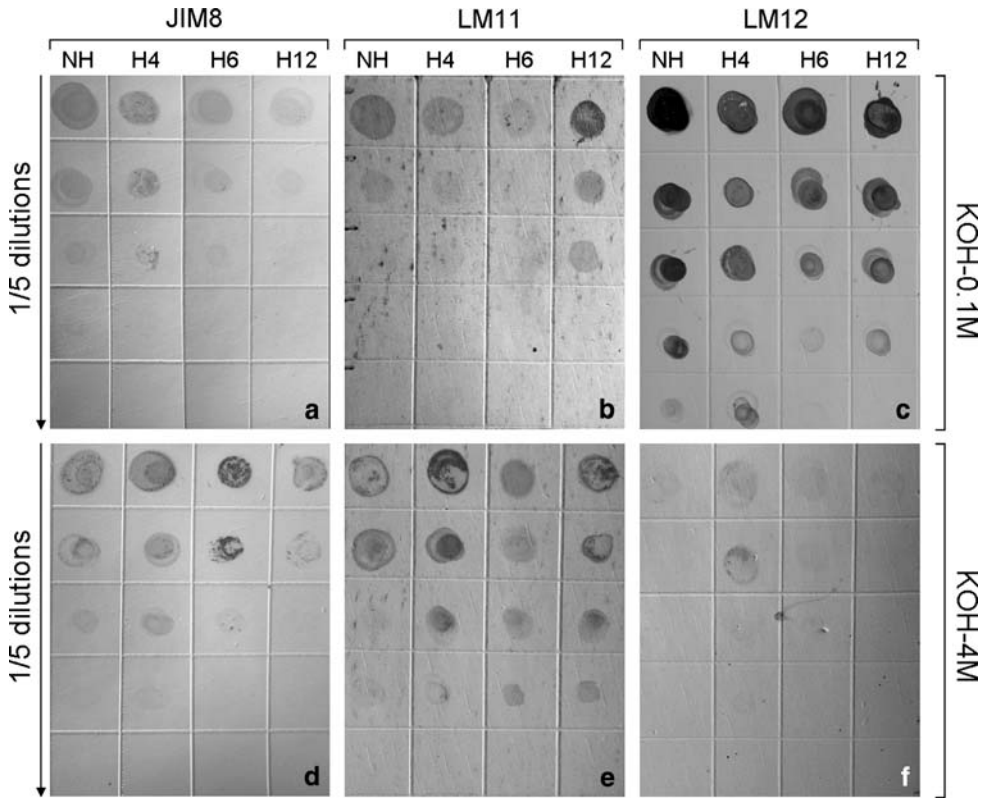

Fig. 11 Immunodot assays of KOH cell wall fractions from NH, H4, H6 and H12 calluses, probed with monoclonal antibodies with specificity for arabinogalactan proteins (JIM8: **a**, **d**), xylan/arabinoxylan (LM11: **b**, **e**) and feruloylates (LM12: **c**, **f**)

increase in M_w is their cross-linking through the formation of dehydroferulates, and that alkali treatment has been reported to prevent this by releasing ester bonded feruloyl groups (Kerr and Fry 2004). Therefore, an alternative explanation for this result could be the increment in alkali resistant phenolic bridges (ether-linked phenolic groups), which would render highly cross-linked AX even after the alkali treatment.

Phenolics have an important function in type II cell walls, as hydroxycinnamic acid derivatives contribute to wall assembly by cross linking polysaccharides through oxidative coupling. Therefore, we tested whether phenolics could contribute to the global tightening in our "stressed" cell walls. FTIR data pointed to an enhanced contribution of phenolics in DCB-habituated cells, as peaks assigned to phenolic ester (1,725 cm^{-1}) and aromatic rings (1,515, 1,600, 1,630 cm^{-1}) were more pronounced. Furthermore, TLC showed interesting changes in phenolic profiles: as described for DCB-habituated barley cultures, there was a shift from ferulic acid-rich walls to *p*-coumaric acid-rich walls (Shedletzky et al. 1992). In addition, in our DCB-habituated maize cells, an enrichment in 5,5 and 8,5 dehydroferulates, and in other compounds with low R_f, which could correspond to trimers or tetramers, was noticed. Therefore, these results indicated a general increase in hydroxycinnamic acid derivatives and in particular, in oxidative coupled derivatives. LM12 immunolocation showed that feruloyl groups were distributed mainly in cell wall areas next to plasmalemma. In conclusion, DCB-habituated maize cells not only showed enrichment in arabinoxylans: they also seemed to have a different GAX structure, together with an enrichment in phenolic compounds, which contributes to its cross-linking.

Other polymers do not seem to make a relevant contribution to modifications in the cell wall architecture of DCB-habituated maize cells. Mannose content was very low in both non-habituated and in habituated cells, so that mannan contribution to DCB-habituation was negligible. Xyloglucan levels were very low too, less than 20 μg mg^{-1} cell wall, and they were even lower in habituated cells. CDTA-extracted pectins were present in a low proportion (lower than 20 μg mg^{-1} cell wall) and did not undergo changes throughout the habituation process. Last, protein content was even lower than in their non-habituated counterparts, as was shown by FTIR spectroscopy, total Kjeldhal nitrogen determination, and immunochemical approaches. It is interesting to note that this reduction affected some groups of proteins, but not others: i.e. LM2 probed AGPs apparently did not vary, whereas JIM8 probed AGPs reduced, as was ascertained using immunolocation and IDAs.

According to Carpita's model (Carpita et al. 2001), type II cell walls are mainly constituted by two domains: a framework of cellulose microfibrils interlaced with tightly adherent β-glucans, GAX of low degrees of arabinosyl substitution and glucomannans; this is then embedded in a

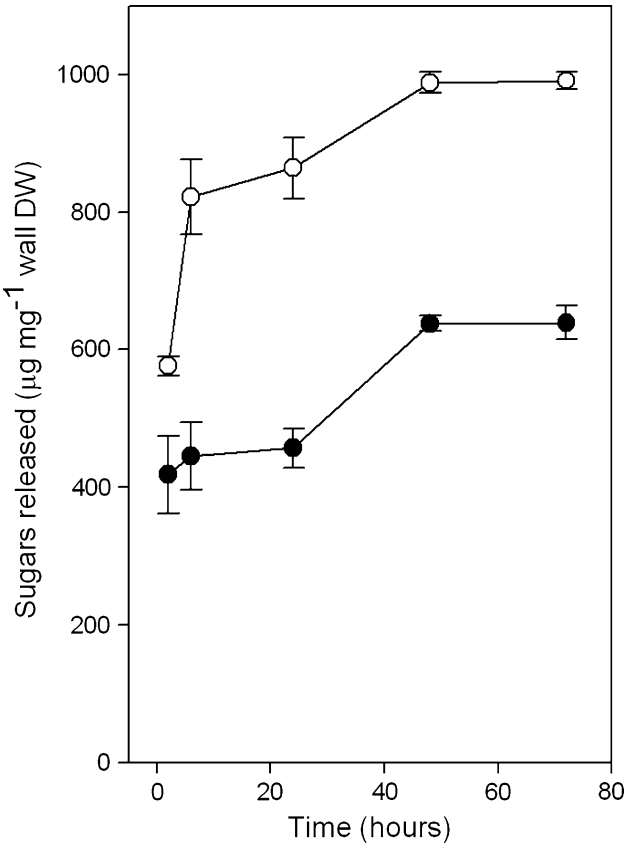

Fig. 12 Cell wall degradability of (*open circle*) NH and (*filled circle*) H12 calluses. Values are mean ± SD of nine measurements

matrix which provides an interstitial domain interconnecting the β-glucan-coated microfibrils, constituted by GAX, which is more highly substituted by arabinosyl residues, additional glucomannan and some pectins. According this model, cell wall porosity would be controlled by the content of GAX with a higher degree of arabinosyl substitution, taking into account that this polysaccharide constitutes the major pore-determining interstitial material between the microfibrils (Carpita et al. 2001). In an interesting experiment conducted in order to study xylanase penetration in wheat endosperm, Beaugrand et al. (2005) found complementary evidence that AXs acts to control pore size, as they observed that this penetration was intrinsically linked to AX degradation, and was facilitated by progressive cell wall disassembly. In DCB-habituated maize cells, cellulose microfibrils would be more interspersed by a larger interstitial AX, which determined the notable increment observed in their pore size, in comparison to non-habituated cells. In contrast, reported cell wall porosity of DCB-habituated barley cells was notably minor, this fact being consistent with a higher content in β-glucan, which would be interspersed between microfibrils, consequently reducing pore size between them.

The observed reduction in swelling capacity of DCB-habituated maize cell walls could be related both to the enrichment in their phenolic component—which would increase cell wall hydrophobicity—and to a hydrogen bonding increase due to AX enhancement, both in concentration and in molecular mass, in an opposite way as that described for expansin action: expansins would lead to an enhancement in cell wall swelling capacity breaking hydrogen bonds to release steric constraint of microfibril movement (Thompson 2005; Yennawar et al. 2006).

Another consequence of the modification in cell wall architecture associated with DCB habituation is the change in cell wall degradability. In this respect, the expectation would be that the reduction in crystalline cellulose and the increase in matrix polysaccharides would contribute to enhanced cell wall degradability. However, cell walls from DCB-habituated maize cells proved to be less susceptible to enzymatic hydrolysis than non-habituated cell walls. The most probable explanation for this result is related to a phenolic-enriched cell wall. Cell wall feruloylation, and particularly increased dimerization of ferulate, has been shown to reduce cell wall degradability by reducing matrix polysaccharide accessibility to hydrolytic enzymes (Grabber 2005 and references therein). Additionally, the enrichment in *p*-coumaric acid of our DCB-habituated cell walls would also contribute to a reduction in their degradability as has been previously reported for ruminal digestibility of some grasses (Burritt et al. 1984).

In summary, maize cell cultures from immature embryos have been successfully habituated to DCB. Habituated cells showed a modified cell wall architecture in which the significant reduction in cellulose content was compensated for by an increment in GAXs, which were of a higher molecular mass, more strongly cell wall bound, and more interlaced by means of phenolic bonds. Other cell wall components do not seem to play a significant role in the habituation process. In contrast to previously described type II cell wall architecture, in DCB-habituated maize cells induced to have reduced cellulose content, β-glucan does not fulfill an important role in the acquisition of functional type II cell wall architecture. As a consequence and in contrast to that previously described, the swelling capacity and wall digestibility of maize habituated cell walls was diminished, whereas pore size became bigger. Future studies need to be conducted in order to examine in greater depth the interaction between GAX and phenolics, and to ascertain the genetic control of these modifications in type II cell wall architecture.

Acknowledgments This work was supported by grants from Junta de Castilla y León (LE 048A07), University of León (ULE-2006-2) and Spanish Science and Innovation Ministry (CGL2008-02470/BOS), and a PhD grant from the FPU program of the Spanish Science and Innovation Ministry to H.M.M. We are grateful to Dr. Paul Knox

for his kind gifts of LM10, LM11 and LM12 antibodies, to Dr. Stephen C. Fry for his kind provision of maize cell cultures and to Denise Phelps for English language correction.

References

Albersheim P, Nevins PD, English PD, Karr A (1967) A method for the analysis of sugars in plant cell wall polysaccharides by gas liquid chromatography. Carbohydr Res 5:340–345

Alonso ML, Alvarez AI, Zapico J (1994) Rapid analysis of free amino-acids in infant foods. J Liq Chromatogr 17:4019–4030

Alonso-Simón A, Encina AE, García-Angulo P, Alvarez JM, Acebes JL (2004) FTIR spectroscopy monitoring of cell wall modifications during the habituation of bean (*Phaseolus vulgaris* L.) callus cultures to dichlobenil. Plant Sci 167:1273–1281

Baron-Epel O, Gharyal PK, Schindler M (1988) Pectins as mediators of wall porosity in soybean cells. Planta 175:389–395

Beaugrand J, Paes G, Reis D, Takahashi M, Debeire P, O'Donohue M, Chabbert B (2005) Probing the cell wall heterogeneity of micro-dissected wheat caryopsis using both active and inactive forms of a GH11 xylanase. Planta 222:246–257

Blumenkrantz N, Asboe-Hansen G (1973) New method for quantitative determination of uronic acids. Anal Biochem 54:484–489

Burritt EA, Bittner AS, Street JC, Anderson MJ (1984) Correlations of phenolic acids and xylose content of cell-wall with in vitro dry-matter digestibility of 3 maturing grasses. J Dairy Sci 67:1209–1213

Carpita NC (1996) Structure and biogenesis of the cell walls of grasses. Annu Rev Plant Physiol Plant Mol Biol 47:445–476

Carpita NC, Gibeaut DM (1993) Structural models of primary cell walls in flowering plants. Consistency of molecular structure with the physical properties of the walls during growth. Plant J 3:1–30

Carpita NC, Defernez M, Findlay K, Wells B, Shoue DA, Catchpole G, Wilson RH, McCann MC (2001) Cell wall architecture of the elongating maize coleoptile. Plant Physiol 127:551–565

Delmer DP (1987) Cellulose biosynthesis. Annu Rev Plant Physiol Plant Mol Biol 38:259–290

Díaz-Cacho P, Moral R, Encina A, Acebes JL, Alvarez J (1999) Cell wall modifications in bean (*Phaseolus vulgaris*) callus cultures tolerant to isoxaben. Physiol Plant 107:54–59

Dische Z (1962) Color reactions of carbohydrates. In: Whistler RL, Wolfrom ML (eds) Methods in carbohydrate chemistry. Academic Press, New York, pp 475–514

Dubois M, Gilles KA, Hamilton JK, Rebers PA, Smith F (1956) Colorimetric method for determination of sugars and related substances. Anal Chem 28:350–356

Encina AE, Moral RM, Acebes JL, Alvarez JM (2001) Characterization of cell walls in bean (*Phaseolus vulgaris* L.) callus cultures tolerant to dichlobenil. Plant Sci 160:331–339

Encina A, Sevillano JM, Acebes JL, Alvarez J (2002) Cell wall modifications of bean (*Phaseolus vulgaris*) cell suspensions during habituation and dehabituation to dichlobenil. Physiol Plant 114:182–191

Fry SC, Willis SC, Paterson AEJ (2000) Intraprotoplasmic and wall-localized formation of arabinoxylan-bound diferulates and larger ferulate coupling-products in maize cell-suspension cultures. Planta 211:679–692

García-Angulo P, Willats WGT, Encina A, Alonso-Simón A, Alvarez JM, Acebes JL (2006) Immunocytochemical characterization of the cell walls of bean cell suspensions during habituation and dehabituation to dichlobenil. Physiol Plant 127:87–99

Grabber JH (2005) How do lignin composition, structure, and cross-linking affect degradability? A review of cell wall model studies. Crop Sci 45:820–831

Grabber JH, Ralph J, Hatfield RD (1998) Severe inhibition of maize wall degradation by synthetic lignins formed with coniferaldehyde. J Sci Food Agric 78:81–87

Iraki NM, Bressan RA, Hasegawa PM, Carpita NC (1989) Alteration of the physical and chemical structure of the primary cell wall of growth limited plant cells adapted to osmotic stress. Plant Physiol 91:39–47

Ishii T (1997) Structure and functions of feruloylated polysaccharides. Plant Sci 127:111–127

Kacurakova M, Wellner N, Ebringerova A, Hromadkova Z, Wilson RH, Belton PS (1999) Characterisation of xylan-type polysaccharides and associated cell wall components by FT-IR and FT-Raman spectroscopies. Food Hydrocoll 13:35–41

Kerr EM, Fry SC (2003) Pre-formed xyloglucans and xylans increase in molecular weight in three distinct compartments of a maize cell-suspension culture. Planta 217:327–339

Kerr EM, Fry SC (2004) Extracellular cross-linking of xylan and xyloglucan in maize cell-suspension cultures: the role of oxidative phenolic coupling. Planta 219:73–83

Kooiman P (1960) A method for the determination of amyloid in plant seeds. Recl Trav Chim Pays Bas Belg 79:675–678

Lorences EP, Fry SC (1991) Absolute measurement of cell expansion in plant cell suspension cultures. Plant Cell Tissue Organ Cult 24:211–215

McCartney L, Marcus SE, Knox JP (2005) Monoclonal antibodies to plant cell wall xylans and arabinoxylans. J Histochem Cytochem 53:543–546

McCleary BV, Codd R (1991) Measurement of $(1 \rightarrow 3),(1 \rightarrow 4)$-β-d-glucan in barley and oats. A streamlined enzymatic procedure. J Sci Food Agric 55:303–312

Murashige T, Skoog F (1962) A revised medium for rapid growth and bio assays with tobacco tissue cultures. Physiol Plant 15:473–497

Nakagawa N, Sakurai N (1998) Increase in the amount of celA1 protein in tobacco BY–2 cells by a cellulose biosynthesis inhibitor, 2, 6-dichlorobenzonitrile. Plant Cell Physiol 39:779–785

Nakagawa N, Sakurai N (2001) Cell wall integrity controls expression of endoxyloglucan transferase in tobacco BY2 cells. Plant Cell Physiol 42:240–244

Pennell R, Knox J, Scofield G, Selvendran R, Roberts K (1989) A family of abundant plasma membrane-associated glycoproteins related to the arabinogalactan proteins is unique to flowering plants. J Cell Biol 108:1967–1977

Pennell RI, Janniche L, Kjellbom P, Scofield GN, Peart JM, Roberts K (1991) Developmental regulation of a plasma membrane arabinogalactan protein epitope in oilseed rape flowers. Plant Cell 3:1317–1326

Sabba RP, Durso NA, Vaughn KC (1999) Structural and immunocytochemical characterization of the walls of dichlobenil-habituated BY-2 tobacco cells. Int J Plant Sci 160:275–290

Saeman JF, Moore WE, Millet MA (1963) Sugar units present. In: Whistler RL (ed) Methods in carbohydrate chemistry. Academic Press, New York, pp 54–69

Shedletzky E, Shmuel M, Delmer DP, Lamport DTA (1990) Adaptation and growth of tomato cells on the herbicide 2, 6-dichlorobenzonitrile leads to production of unique cell walls virtually lacking a cellulose-xyloglucan network. Plant Physiol 94:980–987

Shedletzky E, Shmuel M, Trainin T, Kalman S, Delmer D (1992) Cell wall structure in cells adapted to growth on the cellulose synthesis inhibitor 2, 6-dichlorobenzonitrile. A comparison between two dicotyledonous plants and a gramineous monocot. Plant Physiol 100:120–130

Smallwood M, Yates EA, Willats WGT, Martin H, Knox JP (1996) Immunochemical comparison of membrane-associated and secreted arabinogalactan-proteins in rice and carrot. Planta 198:452–459

Thompson DS (2005) How do cell walls regulate plant growth? J Exp Bot 56:2275–2285

Updegraff DM (1969) Semimicro determination of cellulose in biological materials. Anal Biochem 32:420–424

Vaughn KC (2002) Cellulose biosynthesis inhibitor herbicides. In: Böger P, Wakabayashi K, Hirai K (eds) Herbicide classes in development. Springer, Berlin, pp 139–150

Wells B, Mccann MC, Shedletzky E, Delmer D, Roberts K (1994) Structural features of cell walls from tomato cells adapted to grow on the herbicide 2, 6-dichlorobenzonitrile. J Microsc 173:155–164

Willats WGT, Gilmartin PM, Mikkelsen JD, Knox JP (1999) Cell wall antibodies without immunization: generation and use of de-esterified homogalacturonan block-specific antibodies from a naive phage display library. Plant J 18:57–65

Yennawar NH, Li LC, Dudzinski DM, Tabuchi A, Cosgrove DJ (2006) Crystal structure and activities of EXPB1 (Zea m 1), a β-expansin and group-1 pollen allergen from maize. Proc Natl Acad Sci USA 103:14664–14671